2010-09-03

MD-2 residues tyrosine 42, arginine 69, aspartic acid 122, and leucine 125 provide species specificity for lipid IVA

Jianmin Meng
University of Massachusetts Medical School

Et al.

THE JOURNAL OF BIOLOGICAL CHEMISTRY VOL. 285, NO. 36, pp. 27935–27943, September 3, 2010

MD-2 Residues Tyrosine 42, Arginine 69, Aspartic Acid 122, and Leucine 125 Provide Species Specificity for Lipid IV_A*[S]

Received for publication, April 15, 2010, and in revised form, June 23, 2010 Published, JBC Papers in Press, June 30, 2010, DOI 10.1074/jbc.M110.134668

Jianmin Meng, Joshua R. Drolet, Brian G. Monks, and Douglas T. Golenbock[1]

From the Division of Infectious Diseases and Immunology, University of Massachusetts Medical School, Worcester, Massachusetts 01605

Lipopolysaccharide (LPS) activates the innate immune response through the Toll-like receptor 4 (TLR4)·MD-2 complex. A synthetic lipid A precursor, lipid IV_A, induces an innate immune response in mice but not in humans. Both TLR4 and MD-2 are required for the agonist activity of lipid IV_A in mice, with TLR4 interacting through specific surface charges at the dimerization interface. In this study, we used site-directed mutagenesis to identify the MD-2 residues that determine lipid IV_A species specificity. A single mutation of murine MD-2 at the hydrophobic pocket entrance, E122K, substantially reduced the response to lipid IV_A. Combining the murine MD-2 E122K with the murine TLR4 K367E/S386K/R434Q mutations completely abolished the response to lipid IV_A, effectively converting the murine cellular response to a human-like response. In human cells, however, simultaneous mutations of K122E, K125L, Y41F, and R69G on human MD-2 were required to promote a response to lipid IV_A. Combining the human MD-2 quadruple mutations with the human TLR4 E369K/Q436R mutations completely converted the human MD-2/human TLR4 receptor to a murine-like receptor. Because MD-2 residues 122 and 125 reside at the dimerization interface near the pocket entrance, surface charge differences here directly affect receptor dimerization. In comparison, residues 42 and 69 reside at the MD-2/TLR4 interaction surface opposite the dimerization interface. Surface charge differences there likely affect the binding angle and/or rigidity between MD-2 and TLR4, exerting an indirect influence on receptor dimerization and activation. Thus, surface charge differences at the two MD-2/TLR4 interfaces determine the species-specific activation of lipid IV_A.

Lipopolysaccharide (LPS), also known as endotoxin, activates the innate immune response during Gram-negative bacterial infection. Lipid A, the active component of LPS, anchors LPS to the outer leaflet of the outer membrane of Gram-negative bacteria. When bacteria divide or die, LPS released into local tissue or the circulation can trigger innate immune recognition (1). Lipid A from most species is highly proinflammatory, although certain lipid A molecules and precursors lack stimulatory power. The synthetic precursor of *Escherichia coli* lipid A, tetraacylated lipid IV_A (2) (compound 406), is an agonist in murine cells and a partial agonist in equine cells but is an antagonist in human cells (3).

The Toll-like receptor 4 (TLR4)[2] and MD-2 complex constitute the essential components of a receptor system for LPS (4, 5). CD14, initially believed to be the LPS receptor, is an enhancing component of the LPS receptor (6). The lack of a transmembrane or an intracellular signaling domain led to speculation about an additional LPS receptor component that actually transduces the LPS signal. TLR4 was identified as the signaling component of the LPS receptor, based on positional cloning in mice that fail to respond to LPS (4, 7) and on the finding that TLR4 knock-out cells did not respond to LPS (8). The co-receptor MD-2 is essential for LPS recognition (5), and a single MD-2 point mutation that replaces cysteine 95 with tyrosine (C95Y) completely abolishes LPS responsiveness (9). MD-2 knock-out mice, like TLR4 knock-outs, do not respond to LPS (10). A deficiency in either TLR4 or MD-2 abrogates LPS signaling, whereas a deficiency in CD14 leads to a 100–1000-fold decrease in LPS sensitivity for most proinflammatory genes (*e.g.* TNF-α and IL1β) and the apparent abolishment of response for others (*e.g.* IP-10) (11) but does not abolish LPS signaling. The loss of CD14 therefore differs from the loss of TLR4 or MD-2 in that the presence of CD14 sensitizes cells to the presence of LPS whereas TLR4 or MD-2 are absolutely required for LPS responses.

The co-crystal structure of the human TLR4·MD-2·LPS complex revealed that LPS binds to MD-2 through the LPS acyl chains and the MD-2 hydrophobic pocket (12). Five of the six acyl chains are buried inside the hydrophobic pocket. The sixth lies on the surface above the hydrophobic pocket and, along with the MD-2 Phe-126 and Met-85 loops, interacts with the hydrophobic residues on the C-terminal β-strands (β18–β21) of TLR4 to mediate dimer:dimer assembly of two LPS-liganded TLR4·MD-2 complexes (note: to facilitate an understanding of the data shown in this report, the TLR4, MD-2, LPS molecules in the second TLR4·MD-2·LPS complex will be labeled as TLR4′, MD-2′, LPS′). Hydrogen bonds and ionic interactions are found at the dimerization interface between TLR4, MD-2, and LPS in the co-crystal structure. Surprisingly, the LPS core polysaccharide, which is not required to induce a proinflammatory response, also interacts extensively with TLR4 in the co-crystal structure. Studies with site-directed mutagenesis con-

* This work was supported, in whole or in part, by National Institutes of Health Grants GM54060 (to D. T. G.) and U19 AI084048 (to J. M. and D. T. G.).

[S] The on-line version of this article (available at http://www.jbc.org) contains supplemental Figs. S1–S7 and additional references.

[1] To whom correspondence should be addressed: Division of Infectious Diseases and Immunology, Dept. of Medicine, University of Massachusetts Medical School, 364 Plantation St., LRB 208, Worcester, MA 01605. Fax: 508-856-5463; E-mail: douglas.golenbock@umassmed.edu.

[2] The abbreviations used are: TLR4, Toll-like receptor 4; h, human; m, mouse; PDB, Protein Data Bank.

firmed that Phe-126 on human MD-2 (hMD-2) is essential for receptor dimerization (13) and demonstrated that hydrophobic residues on hMD-2 and human TLR4 (hTLR4) are required for receptor activation (14).

We previously demonstrated that ionic interactions at the dimerization interface play an essential role in lipid IV_A activation (15). Mouse TLR4 (mTLR4) is required for the species-specific activation of lipid IV_A because, in the presence of mouse MD-2 (mMD-2), one phosphate on lipid IV_A can interact with a positively charged patch on the opposing mTLR4 (at the dimerization interface) to trigger dimerization. This positively charged patch on mTLR4 is replaced with a negatively charged patch on hTLR4, with the result that human TLR4 does not respond to lipid IV_A (15).

In this study, we used site-directed mutagenesis to swap surface charges between human and mouse MD-2 to identify residues on MD-2 that account for lipid IV_A species specificity. We produced five mutations in both murine and human MD-2 at residues 42, 69, 58, 122, and 125 designed to swap surface charges between the two species. We then tested whether these charge changes interconverted the human and mouse phenotypic responses to lipid IV_A. We found that the E122K mutation was sufficient to abrogate the lipid IV_A response by murine MD-2 but that the K122E mutation alone was not sufficient to induce a response by human MD-2; simultaneous mutations of K125L, R69G, and Y42F also were required for an hMD-2 response. Furthermore, when the hMD-2 quadruple mutant was introduced to HEK293 cells with the hTLR4 E369K/Q436R double mutant, a full lipid IV_A response was observed, indicating that the hTLR4·hMD-2 receptor has been converted to a mouse phenotype after these mutations. Conversely, lipid IV_A inhibited LPS responses when the mMD-2 E122K mutant was introduced to HEK293 cells with the mTLR4 K367E/S386K/R434Q mutant, suggesting a conversion of the murine receptor to a human phenotype after these mutations. Thus, unique MD-2 surface charges at the two MD-2/TLR4 interfaces determine the role of MD-2 in lipid IV_A activation.

EXPERIMENTAL PROCEDURES

Mutagenesis and Luciferase Assay—Synthetic lipid IV_A was a gift from Dr. Shoichi Kusumoto (Osaka University, Osaka, Japan). LPS from *E. coli* strain O111:B4 (Sigma) was repurified by a repeat phenol-chloroform extraction (16). The wild type (WT) hMD-2 and mMD-2 constructs in pEFBOS vector (a gift of Dr. Kensuke Miyake, Saga Medical School, Nabeshima, Japan) were used as the PCR template for QuikChange site-directed mutagenesis under the manufacturer's instruction (Stratagene). The hMD-2 mutants that contain one or more of the five mutations, F42Y, N58K, G69R, E122K, and L125K, were engineered from the hMD-2 WT construct, and the mMD-2 mutants that contain one or more of the five mutations, Y42F, K58N, R69G, K122E, and K125L were engineered from the mMD-2 WT construct. All mutations were verified by DNA sequencing (Genewiz, Inc., South Plainfield, NJ).

The effects of these mutations on LPS and lipid IV_A signaling were tested in HEK293 cells by transient transfection. HEK293 cells were plated in 96-well plates at a density of 20,000 cells/well. The next day, cells were transfected with: (i) one of the

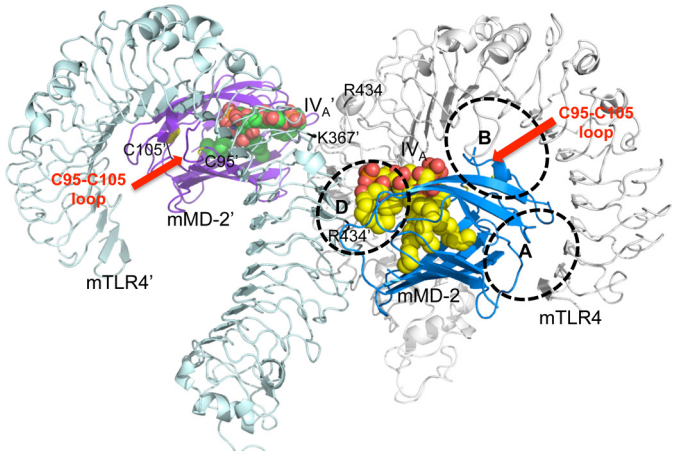

FIGURE 1. **Dimeric mTLR4·mMD-2·lipid IV_A model.** A dimeric mTLR4·mMD-2·lipid IV_A model was produced as described (15). The A patch, B patch, and the dimerization interface are *circled* with *dashed lines* and labeled as *A*, *B*, and *D*, respectively. The mTLR4, mMD-2, and lipid IV_A from the second mTLR4·mMD-2·lipid IV_A complex are labeled as mTLR4′, mMD-2′, and lipid IV_A′ to differentiate these proteins from those of the first mTLR4·mMD-2·lipid IV_A complex. Residues Arg-434 on the first mTLR4·mMD-2· lipid IV_A complex, and Lys-367′, Arg-434′, Cys-95′, and Cys-105′ on the second mTLR4·mMD-2·lipid IV_A complex are labeled. The Cys-95–Cys-105 loops are indicated by the *red arrow* and labeled. Color scheme: mTLR4, *white ribbon*; mMD-2, *blue ribbon*; lipid IV_A, *yellow spheres*; mTLR4′, *blue-white ribbon*; mMD-2′, *purple ribbon*; lipid IV_A′, *green spheres*.

$hTLR4^{YFP}$ constructs (E369K/Q436R, E369K/K388S/Q436R, or a WT control), or one of the $mTLR4^{YFP}$ constructs (K367E/R434Q, K367E/S386K/R434Q, or a WT control); (ii) one of the hMD-2 or mMD-2 mutants; (iii) an NF-κB-luciferase plasmid (17); and (iv) the *Renilla*-luciferase plasmid. The next day, the medium was changed to fresh complete DMEM without serum, and cells were stimulated with the indicated concentrations of LPS/lipid IV_A. After overnight stimulation, the supernatants were removed, and firefly-luciferase activity was measured in cell lysates. *Renilla*-luciferase was used for normalization.

For inhibition assays in HEK293 cells, HEK293 cells were plated as described above and transfected with: (i) one of the mMD-2 mutants (E122K or F42Y/G69R/E122K/L125K) or a WT control; (ii) one of the mTLR4 mutants (K367E/R434Q or K367E/S386K/R434Q) or a WT control; (iii) an NF-κB-luciferase reporter construct; and (iv) a *Renilla*-luciferase reporter construct. The next day, 1000 ng/ml lipid IV_A was added to selected wells, and after 1 h of incubation, 100 ng/ml LPS was added to the experimental wells. After overnight stimulation, NF-κB-luciferase was measured in cell lysates as described above. *Renilla*-luciferase was used to normalize NF-κB-luciferase.

RESULTS

Human and Mouse MD-2 Have Different Surface Charges Near the Entrance of the Hydrophobic Pockets—According to our previous model of dimeric mTLR4/mMD-2/lipid IV_A (Fig. 1) (15), lipid IV_A packs shallowly in the mMD-2 hydrophobic pocket with the diglucosamine backbone tilted toward the Cys-95–Cys-105 loop opposite the dimerization interface (12, 15). This position lifts the 4′-phosphate of lipid IV_A up from the hydrophobic pocket so that it can interact with the two positively charged residues, Lys-367 and Arg-434, on the opposing mTLR4 (Fig. 1) to trigger dimerization. (Residues on the second

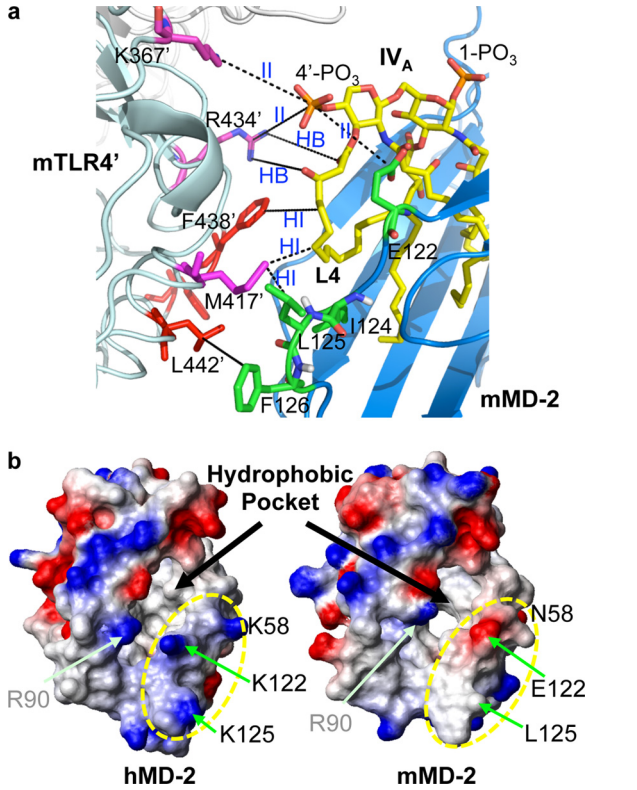

FIGURE 2. **Electrostatic surface charges are different between hMD-2 and mMD-2 near the hydrophobic pocket entrance.** *a*, zoomed-in view of the dimerization interface of the mTLR4/mMD-2/lipid IV_A model. Molecules and residues from the second TLR4·MD-2·lipid IV_A complex are labeled with "′" to differentiate from those of the first TLR4·MD-2·lipid IV_A complex. Hydrophobic interactions, hydrogen bonds, and ionic interactions are indicated by *dashed lines* and labeled in *blue* as *HI*, *HB*, and *II*, respectively. The fourth acyl chain of lipid IV_A is labeled as L4. Color scheme: mMD-2, *blue ribbon*; lipid IV_A, *yellow sticks*; mTLR4′, *blue-white ribbon*. Residues on mTLR4′ are colored in *red* or *magenta* and labeled; residues on mMD-2 are colored in *green* and labeled. The electrostatic surface charges were calculated for hMD-2 and mMD-2 in MolMol (21). *b*, surface charges near the hydrophobic pocket entrance of hMD-2 (*left*) and mMD-2 (*right*). Color scheme: negatively charged surface, *red*; positively charged surface, *blue*; and noncharged surface, *white*. Surfaces that differ between hMD-2 and mMD-2 are *circled* in *yellow* and labeled. Selective surfaces that are common between hMD-2 and mMD-2 are labeled in *gray*.

TLR4/MD-2/lipid IV_A molecule are designated "′") Because these two residues are replaced with the negatively charged Glu-369′ and Gln-436′ in hTLR4, lipid IV_A does not activate proinflammatory responses when hTLR4 is present. Hence, the surface charges of TLR4 at the dimerization interface determine the role of TLR4 in lipid IV_A recognition.

Hydrophobic interactions and hydrogen bonds were observed at the dimerization interface of the lipid IV_A activation model (Fig. 2*a*). However, because of a reduction of two acyl chains from hexaacylated LPS to tetraacylated lipid IV_A, hydrophobic interactions with the acyl chains were reduced at the dimerization interface in the mTLR4/mMD-2/lipid IV_A model. As shown in Fig. 2*a*, only the upper portion of the fourth acyl chain on lipid IV_A was expected to be involved in hydrophobic interactions with mMD-2 and mTLR4 at the dimerization interface. In comparison, hydrophobic interactions between mMD-2 and mTLR4 at the dimerization interface in the mTLR4·mMD-2·lipid IV_A model were expected to be similar to those in the hTLR4·hMD-2·LPS co-crystal structure (12), because virtually all hydrophobic residues on MD-2 and TLR4 essential for receptor dimerization (13, 14) are conserved between the two species (12). In addition, mMD-2 has the hydrophobic Leu-125 in place of Lys-125 in hMD-2 (Fig. 2*a*), which likely enhanced hydrophobic interactions between mMD-2 and mTLR4 at the dimerization interface. Similarly, hydrogen bonds between Arg-434′ on mTLR4 and the hydroxyl group on the fourth acyl chain of lipid IV_A (Fig. 2*a*) contributed to the stabilization of the mTLR4/mMD-2/lipid IV_A dimer.

Comparison of the electrostatic surface charges for hMD-2 and mMD-2 (13, 18) revealed differences near the entrance of the hydrophobic pockets (Fig. 2*b*). Human MD-2 has positively charged Arg-90 and Lys-122 at the hydrophobic pocket entrance, whereas mMD-2 has positively charged Arg-90 but negatively charged Glu-122 at the pocket entrance. Human MD-2 has positively charged Lys-125 at the dimerization interface close to the pocket entrance, whereas mMD-2 has hydrophobic Leu-125 at this position. A little further away from the pocket entrance, hMD-2 has positively charged Lys-58 on the β4 strand that has been implicated in lipid IV_A discrimination (19), whereas mMD-2 has negatively charged Asn-58 at this position. Because the acyl chains of LPS bind to the MD-2 hydrophobic pocket, and the diglucosamine backbone of LPS sits next to the pocket entrance (12, 13), modifications of MD-2 surface charges at residues 122, 125, and 58 likely affect lipid binding and directly influence lipid IV_A species specificity.

E122K Mutation on mMD-2 Nearly Eliminated Lipid IV_A Responsiveness—To determine whether any of these surface charge differences alter the response to lipid IV_A, we engineered MD-2 mutants that swapped surface charges between the human and murine analogs. The effects of these mutations were measured with the luciferase assay.

N58K, E122K and L125K mutants were created by site-directed mutagenesis from WT mMD-2 expressed in the pEFBos vector. These single substitutions from the native mouse residues to their human counterparts did not affect LPS signaling (Fig. 3*a*), suggesting that these mutations did not disrupt the structural motif essential for LPS signaling. In comparison, E122K substantially reduced lipid IV_A responsiveness (Fig. 3*b*), indicating that Glu-122 at the pocket entrance is essential for mMD-2 to respond to lipid IV_A.

Mutations K122E and K125L Increased the Human MD-2 Response to Lipid IV_A—We next examined whether E122K was sufficient to convert hMD-2·mTLR4 from a lipid IV_A nonresponder to a responder. The single mutants K58N and K125L were used as controls, and the effects were measured as described. LPS responsiveness was not significantly affected by these mutations (Fig. 3*c*), indicating that they did not disrupt the structural motif essential for LPS signaling. Surprisingly, although the K58N mutation did not confer lipid IV_A responsiveness to hMD-2, the K125L mutation conferred weak lipid IV_A responsiveness to hMD-2. In contrast, the K122E mutation conferred strong lipid IV_A responsiveness to hMD-2 (although not to the level of mMD-2). These data suggest that surface charge differences at residues 122 and 125 participate in lipid IV_A discrimination.

Human and Murine MD-2 Have Different Surface Charges at the A Patch That Physically Associates with TLR4 in the Monomeric MD-2·TLR4 Complex—In the absence of ligand, MD-2 forms a high-affinity complex with TLR4 through interactions

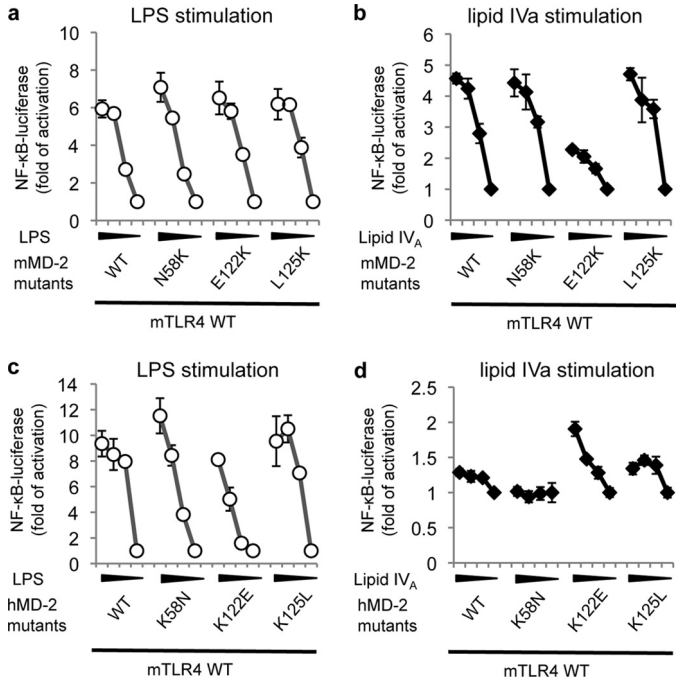

FIGURE 3. **Glu-122 and Leu-125 on mMD-2 are essential for lipid IV_A responsiveness.** HEK293 cells were transiently transfected with: (i) one of mMD-2 (*a* and *b*) or hMD-2 (*c* and *d*) single mutants near the hydrophobic pocket entrance; (ii) mTLR4 WT construct; (iii) a NF-κB luciferase reporter construct; and (iv) a *Renilla*-luciferase reporter construct. The next day, cells were stimulated with 1000 ng/ml, 100 ng/ml, 10 ng/ml, or 0 ng/ml LPS (*a* and *c*) or lipid IV_A (*b* and *d*) overnight. Supernatants were then removed, and NF-κB-luciferase was measured in cell lysates. The luciferase shown has been normalized by *Renilla*-luciferase. The data shown are representative of one experiment that was repeated a total of four times.

at the A and B patches (Figs. 1 and 4, *a* and *b*) (12, 13). The A patch had more interactions in the human complex (Fig. 4*a*), whereas the B patch had more interactions in the mouse complex (Fig. 4*b*). Because a stable TLR4·MD-2 complex is still observed in the absence of intact B patch interactions (13), the A patch interactions between MD-2 and TLR4 likely play a dominant role in the formation of TLR4·MD-2 complex. Surface features at the B patch were quite similar between human and mouse MD-2 (supplemental Fig. 1*a*) and between human and mouse TLR4 (supplemental Fig. 1*b*). It is likely that the differences are a secondary effect of different A patch interactions between the two species.

A delicate interaction network was observed at the A patch of both the human (Fig. 4*c*) and mouse (Fig. 4*d*) TLR4·MD-2 complexes in the co-crystal structures (PDB codes 3FXI and 2Z64) (12, 13). Positive residues Arg-68 and Lys-109, which are conserved between hMD-2 and mMD-2, were involved in extensive hydrogen bonds and ionic interactions with neighboring TLR4 residues at the A patch of the human and mouse complexes (Fig. 4, *c* and *d*). An extra hydrogen bond was found in the human complex between the hydroxyl group of Tyr-42 on hMD-2 and the carboxyl oxygen of Phe-42 on hTLR4 (Fig. 4*c*). This hydrogen bond was absent in the mouse complex because mMD-2 has Phe-42 that lacks the hydroxyl group on the aromatic ring (Fig. 4*d*). Because Tyr-42 resides on the β3 strand of MD-2 (Fig. 4*a*), this extra hydrogen bond between hMD-2 and hTLR4 likely helps to orient the overall conformation of the human complex. For example, it may modify the tilt angle and/or rigidity between hMD-2 and hTLR4 to disfavor dimerization so that extra forces are required to trigger dimerization.

Human and murine MD-2 also differ in electrostatic surface charges at the A patch (Fig. 4*e*). Aside from positively charged Arg-68 and Lys-109 present in both species, the hMD-2 surface also contains positively charged Arg-69 and the amino group of Tyr-42. In mMD-2, Arg-69 is replaced with the noncharged Gly-69, and Tyr-42 is replaced with the more hydrophobic Phe-42, whose amino group does not lie on the surface. Thus, hMD-2 is more positively charged than mMD-2 at the A patch. Consistently, hTLR4 is more negatively charged at the A patch than mTLR4 (supplemental Fig. 1*c*). Because A patch interactions between MD-2 and TLR4 are mainly ionic (Fig. 4, *c* and *d*), the increased positive charges on hMD-2 likely result in a hMD-2·hTLR4 complex that is more tightly bound at the A patch. Thus, a major difference between hMD-2 and mMD-2 at the A patch arises from two residues, 69 and 42, which permit additional interactions within the human MD-2·TLR4 complex that may affect binding angle and/or rigidity between hMD-2 and hTLR4 to disfavor dimerization in the absence of strong agonists such as *E. coli* LPS.

Mutations R69G and Y42F Increased Human MD-2 Response to Lipid IV_A—To determine whether residues 69 and 42 play a role in lipid IV_A discrimination, we swapped charges at these residues between hMD-2 and mMD-2 and measured the effects on LPS/lipid IV_A stimulation as described. Although the F42Y and G69R mutations on mMD-2 did not affect LPS (Fig. 5*a*) or lipid IV_A signaling (Fig. 5*b*), the reverse mutations (R69G and Y42F) on hMD-2 substantially increased lipid IV_A responsiveness (Fig. 5*d*), indicating that additional interactions at the A patch resulting from Tyr-42 and Arg-69 impaired lipid IV_A responsiveness. Thus, lipid IV_A activation of MD-2 is influenced by interactions at both the dimerization interface and the opposite A patch, which physically associates MD-2 with TLR4.

Mutations of Y42F, R69G, K122E, and K125L, in Combination, Converted the Human MD-2 Nonresponse to Lipid IV_A to the Full Mouse-like Response—To examine whether mutations at the dimerization interface and the A patch have a cumulative effect on lipid IV_A signaling, we engineered hMD-2 double mutants that contain pairwise combinations of the five mutations. All mutants retained their ability to respond to LPS (supplemental Fig. 2*a*), indicating that the structural motifs essential for LPS responsiveness are intact in these mutants. However, the magnitudes of the responses were different: hMD-2 responded to lipid IV_A with double mutants containing either K122E or R69G, but the response was higher in the double mutant R69G/K122E (supplemental Fig. 2*b*). This confirms that although Y42F and K125L play a role in responding to lipid IV_A, K122E and R69G are required for a complete LPS-mimetic activity of lipid IV_A.

High order mutants that contain three or four of the five mutations were further engineered by site-directed mutagenesis. Similar to other hMD-2 mutants, the LPS responsiveness remained similar after these mutations (supplemental Fig. 3*a*), suggesting that these mutations did not disrupt the structural motif essential for LPS signaling. However, the lipid IV_A responses were dependent on the

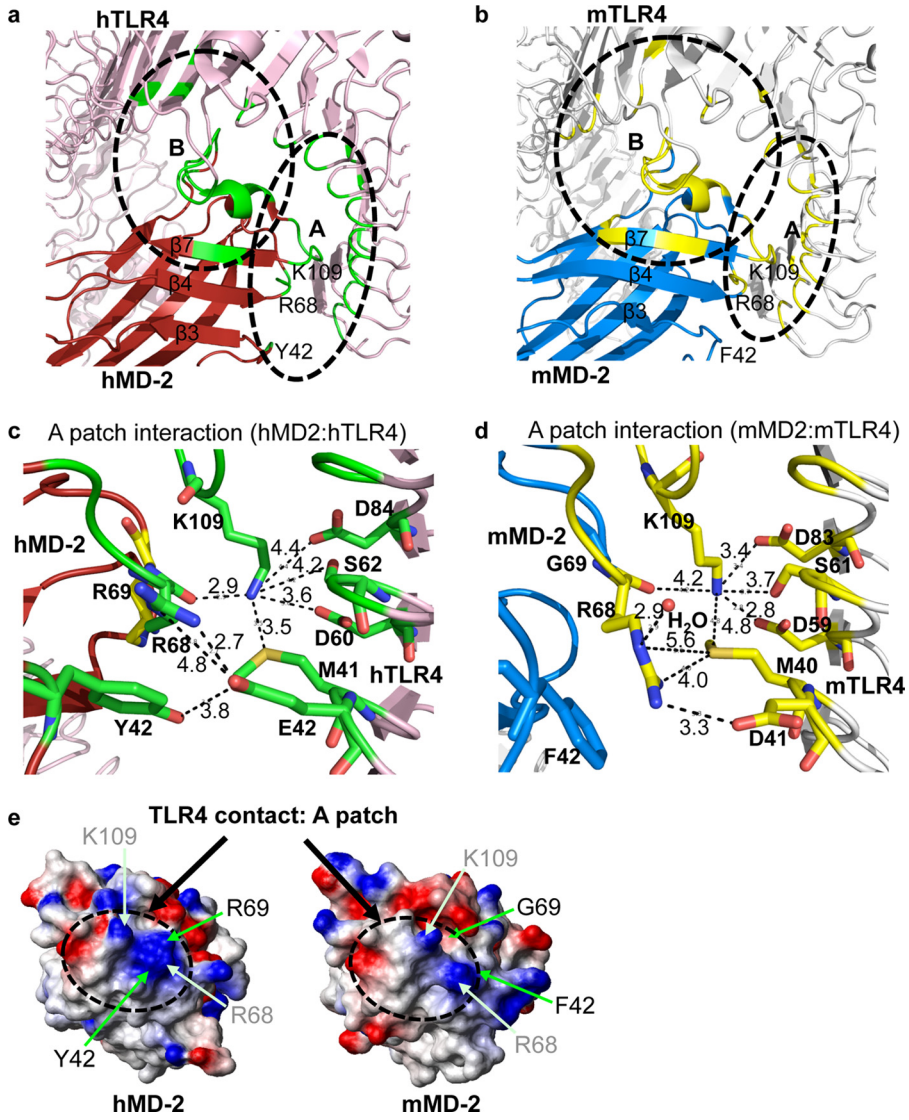

FIGURE 4. **Electrostatic surface charges are different between hMD-2 and mMD-2 at the A patch that physically associates with TLR4.** The monomeric TLR4·MD-2 complexes subtracted from the co-crystal structures (PDB codes 2Z64 and 3FXI) (12, 13) are shown in *a* and *b*. The hMD-2/hTLR4 interfaces (*a*) are colored in *green*, and the mMD-2/mTLR4 interfaces (*b*) are colored in *yellow*. The A and B patches are *circled* and labeled as *A* and *B*, respectively, in *a* and *b*. The β3, β4, and β7 strands on MD-2 are labeled. Zoomed-in views of the A patch interactions are shown in *c* for the human complex, and *d* for the mouse complex. Residues involved in MD-2/TLR4 interactions are shown as *green sticks* in *c* for the human complex and *yellow sticks* in *d* for the mouse complex. Hydrogen bonds and ionic interactions are shown in *dashed lines* in *c* and *d*, with the distances labeled. Color scheme: hTLR4, *pink ribbon*; hMD-2, *brown*; mTLR4, *white ribbon*; mMD-2, *blue ribbon*. The electrostatic surface charges at the A patch are shown in *e*. Negatively charged surface, *red*; positively charged surface, *blue*; noncharged surface, *white*. Surfaces that differ between hMD-2 and mMD-2 are circled in *yellow*, with the residues labeled in *black* in *e*. Surfaces that are common between hMD-2 and mMD-2 are labeled in *gray* in *e*.

mutation (supplemental Fig. 3*b*). There was no significant increase in lipid IV_A response to the triple mutants Y42F/K122E/K125L and K58N/K122E/K125L, which lack the R69G mutation. However, substantial gain of function was observed for the triple mutant R69G/K122E/K125L and the quadruple mutant K58N/R69G/K122E/K125, and the biggest increase was observed for the quadruple mutant Y42F/R69G/K122E/K125L, underscoring the roles of all four mutations in lipid IV_A activation.

Two hMD-2 mutants, R69G/K122E and Y42F/R69G/K122E/K125L, were compared directly with the WT hMD-2 construct for responsiveness to LPS (Fig. 6*a*) or lipid IV_A (Fig. 6*b*). As the number of mutations increased, the responsiveness to lipid IV_A increased. Conversely, when the reverse mutations were introduced to mMD-2 in combination, the lipid IV_A responsiveness was reduced after the G69R/E122K and F42Y/G69R/E122K/L125K mutations (Fig. 6*d*), whereas LPS responsiveness remained unchanged (Fig. 6*c*). (The full list of mMD-2 mutants is shown in Supplemental Figs. 4 and 5.) These results confirm that the four residue differences between hMD-2 and mMD-2, *i.e.* Tyr-42/Phe-42, Arg-69/Gly-69, Lys-122/Glu-122, and Lys-125/Leu-125, all contribute to lipid IV_A discrimination.

In summary, by swapping surface charges between hMD-2 and mMD-2, we demonstrated that Glu-122 is required for mMD-2 to respond to lipid IV_A. Therefore, negative charges conveyed by Glu-122 at the pocket entrance are essential for mMD-2 to respond positively to lipid IV_A stimulation. However, gain of negative charges at the pocket entrance alone (from the K122E mutation) are not sufficient to confer full response to hMD-2 against lipid IV_A stimulation. Gain of hydrophobic surface from the K125L mutation near the dimerization surface (12) and loss of positive charges at the A patch from the R69G and Y42F mutations also are required to convert the mTLR4·hMD-2 complex from a lipid IV_A nonresponder to a lipid IV_A responder. Thus, interactions at the dimerization interface and at the A patch that physically associates MD-2 with TLR4 cumulatively determine the role of MD-2 in the species-specific activation of lipid IV_A.

Lipid IV_A Activated the Mutant hTLR4 (E369K/Q436R)·hMD-2 (Y42F/R69G/K122E/K125L) Complex—We previously demonstrated that, in the presence of mMD-2, hTLR4 gained lipid IV_A responsiveness after the E369K/Q436R mutation or the E369K/K388S/Q436R mutation (15). To test whether the combined mutations of hTLR4 and hMD-2 could convert the human LPS receptor into a mouse phenotype, we co-transfected the hMD-2 mutant (Y42F/R69G/K122E/K125L) with one of the hTLR4 mutants (E369K/Q436R or E369K/K388S/Q436R) and measured activation. The hMD-2 double mutant R69G/K122E was also included in this experiment because it increased lipid IV_A responsiveness more than any other single or double mutant.

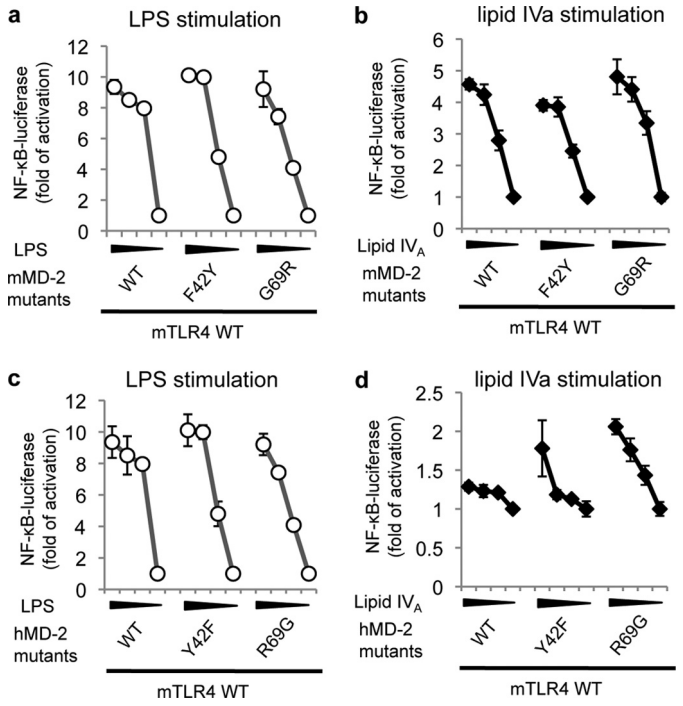

FIGURE 5. **Human MD-2 gained weak lipid IV_A responsiveness after the Y42F or R69G mutation.** HEK293 cells were transiently transfected with: (i) one of the hMD-2 or mMD-2 single mutant at the A patch; (ii) a WT mTLR4 construct; (iii) a NF-κB luciferase reporter construct; and (iv) a *Renilla*-luciferase reporter construct. After overnight transfection, cells were stimulated with 1000 ng/ml, 100 ng/ml, 10 ng/ml, or 0 ng/ml LPS (*a* and *c*) or lipid IV_A (*b* and *d*). The next day, supernatants were removed, and NF-κB-luciferase activity was measured in cell lysates. The luciferase shown has been normalized by *Renilla*-luciferase. The data shown are representative of one experiment that was repeated a total of four times.

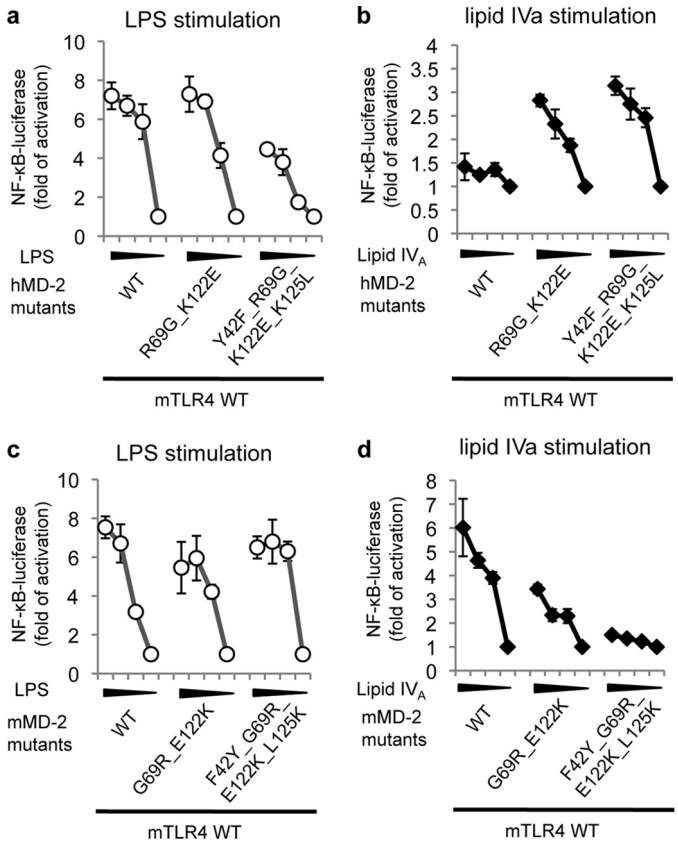

FIGURE 6. **Human MD-2 gained a full lipid IV_A response after the combined mutations of Y42F/R69G/K122E/K125L.** HEK293 cells were transfected with: (i) one of the following MD-2 constructs, hMD-2 WT, hMD-2 R69G/K122E mutant, hMD-2 Y42F/R69G/K122E/K125L mutant, mMD-2 WT, mMD-2 G69R/E122K mutant, mMD-2 F42Y/G69R/E122K/L125K mutant; (ii) a mTLR4 WT construct; (iii) a NF-κB luciferase reporter construct; and (iv) a *Renilla*-luciferase reporter construct. After overnight transfection, cells were stimulated with 1000 ng/ml, 100 ng/ml, 10 ng/ml, or 0 ng/ml LPS (*a* and *c*) or lipid IV_A (*b* and *d*). The next day, supernatants were removed, and NF-κB-luciferase activity was measured in cell lysates. The luciferase shown has been normalized by *Renilla*-luciferase. The data shown are representative of one experiment that was repeated a total of four times.

The LPS response in all of the mutant hTLR4·hMD-2 complexes was approximately half of the response of the WT human complex (Fig. 7*a*), indicating that some surface features essential for an optimal LPS response were lost in the hTLR4·hMD-2 complexes after these mutations were introduced. However, the lipid IV_A response in the mutants was high and dose-dependent, unlike the WT hTLR4·hMD-2 complex that did not respond to lipid IV_A (Fig. 7*b*). These results suggest that the charge reversals at the dimerization interface of hTLR4 and the pocket entrance and at the A patch of hMD-2 are sufficient to convert the human LPS receptor response to a mouse phenotype. All four mutations on hMD-2 must be required because use of the hMD-2 double mutant (R69G/K122E) along with the hTLR4 mutant did not restore lipid IV_A response. Thus, the negative surface of hTLR4 at the dimerization interface, and the more positively charged surface on hMD-2 at the pocket entrance and at the A patch, determine the roles of hTLR4 and hMD-2 in the species-specific activation of lipid IV_A.

Lipid IV_A Inhibited LPS Responses in the Mutant mTLR4 (K367E/S386K/R434Q)·mMD-2 (E122K) Complex—As described above, by grafting positively charged residues to hTLR4 and negatively charged or noncharged residues to hMD-2, we converted the hTLR4·hMD-2 complex to a murine phenotype. To examine the converse, we co-transfected mutant mTLR4 constructs (K367E/R434Q or K367E/S386K/R434Q) with mutant mMD-2 constructs (E122K or F42Y/G69R/E122K/L125K) and tested the lipid IV_A responsiveness.

LPS activated all combinations of mutant mTLR4·mMD-2 complexes (Fig. 8, *black bars*), indicating that the four mutant combinations maintained the structural features required for LPS signaling. In contrast, lipid IV_A did not activate the mutant mTLR4·mMD-2 complexes (Fig. 8, *open bars*), indicating that the loss of positive charge at the dimerization interface of mTLR4 and the loss of negative charge at the hydrophobic pocket entrance of mMD-2 prevented the normal murine lipid IV_A response. Furthermore, when lipid IV_A was incubated with the cells prior to LPS stimulation, lipid IV_A blocked LPS signaling (Fig. 8, *gray bars*). This result suggests that the charge reversals were sufficient to convert the mouse receptor to a human phenotype. Thus, positive charges at the dimerization interface of mTLR4 and negative charges at the pocket entrance of mMD-2 define the roles of mTLR4 and mMD-2 in the species-specific activation of lipid IV_A.

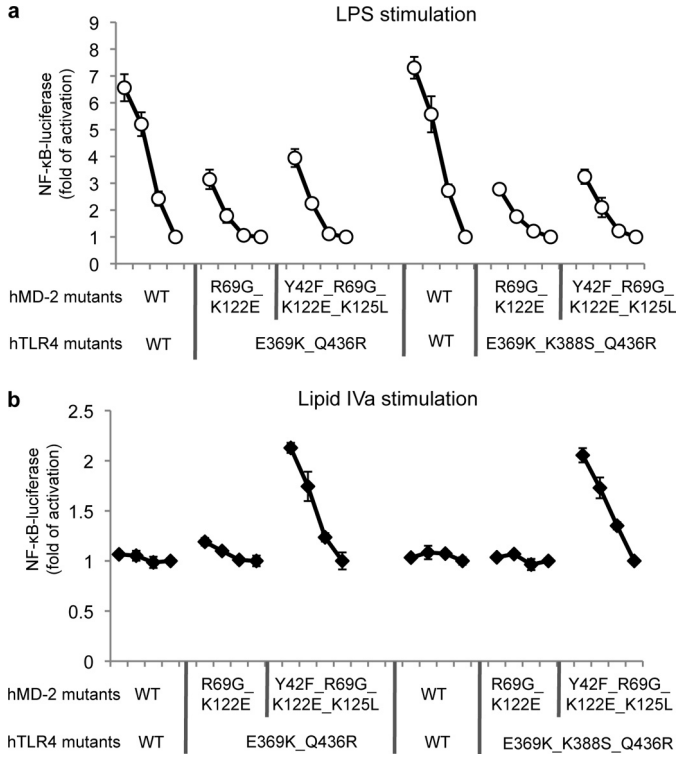

FIGURE 7. **Lipid IV_A activates the hTLR4 (E369K/Q436R or E369K/K388S/Q436R mutant) and hMD-2 (Y42F/R69G/K122E/K125L mutant) complex.** HEK293 cells were plated on 96-well plate overnight. Cells were then transfected with (i) one of the three hMD-2 constructs: WT, R69G/K122E, and Y42F/R69G/K122E/K125L; (ii) one of the hTLR4 constructs: WT, E369K/Q436R, and E369K/K388S/Q436R; (iii) an NF-κB luciferase reporter construct; and (iv) a *Renilla*-luciferase reporter construct. The next day, cells were stimulated with 1000 ng/ml, 100 ng/ml, 10 ng/ml, or 0 ng/ml LPS (*a*) or lipid IV_A (*b*) overnight. Supernatants were then removed, and NF-κB-luciferase was measured in cell lysates. The luciferase shown has been normalized by *Renilla*-luciferase. The data shown are representative of one experiment that was repeated a total of four times.

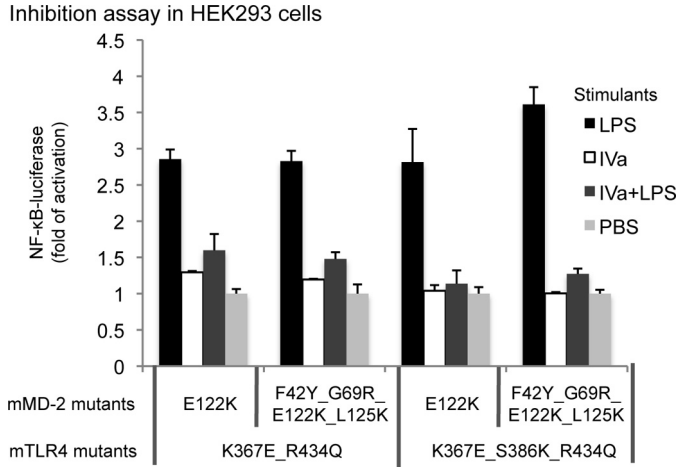

FIGURE 8. **Lipid IV_A inhibits LPS responses in the mutant mTLR4·mMD-2 complexes.** HEK293 cells were plated on a 96-well plate overnight. Cells were then transfected with (i) one of the mMD-2 mutants, E122K or F42Y/G69R/E122K/L125K; (ii) one of the mTLR4 mutants, K367E/R434Q or K367E/S386K/R434Q; (iii) an NF-κB luciferase reporter construct, and (iv) a *Renilla*-luciferase reporter construct. The next day, selected wells of cells were incubated with 1 μg/ml lipid IV_A for 1 h. LPS was then added to selected wells at a concentration of 100 ng/ml. After overnight of stimulation, supernatants were removed, and NF-κB-luciferase was measured in cell lysates. The luciferase shown has been normalized by *Renilla*-luciferase. Data are one representative figure of four repeating experiments.

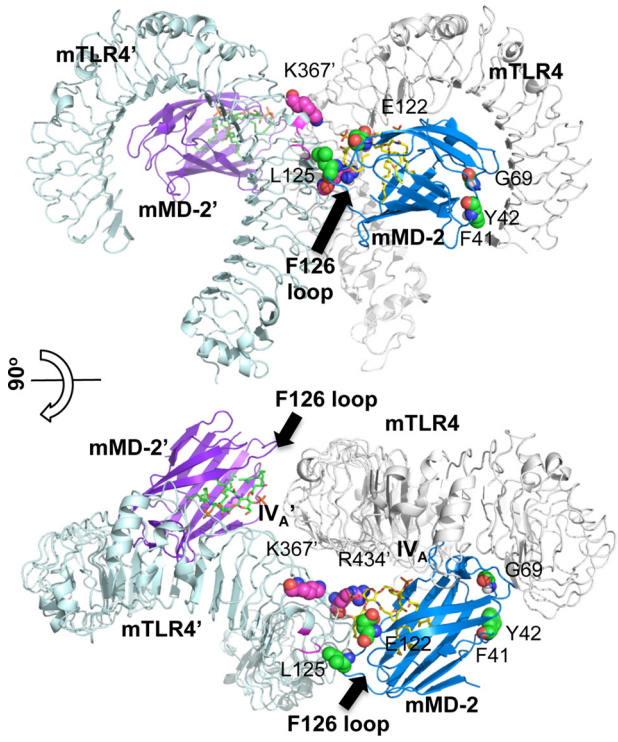

FIGURE 9. **The four key residues on mMD-2, Glu-122, Leu-125, Gly-69 and Tyr-42, reside at the dimerization interface and the A patch in the dimeric mTLR4·mMD-2·lipid IV_A model.** A dimeric mTLR4·mMD-2·lipid IV_A model (15) is shown in two perpendicular views. The essential residues, Lys-367′ and Arg-434′ on mTLR4′, and Glu-122, Leu-125, Gly-69, and Tyr-42 on mMD-2 are labeled and shown as *spheres*. The Phe-126 loop is indicated by the *black arrow* and *labeled*. Phe-41 is labeled according to its atomic position. Color scheme: mTLR4, *white ribbon*; mMD-2, *blue ribbon*; lipid IV_A, *yellow sticks*; mTLR4′, *blue-white ribbon*; mMD-2′, *purple ribbon*; lipid IV_A′, *green sticks*.

DISCUSSION

Lipid IV_A is an agonist in rodent cells but an antagonist in human cells (15). Both mTLR4 and mMD-2 are required for the LPS-mimetic activity of lipid IV_A (15). The essential role of mTLR4 in lipid IV_A activation arises from its unique surface charges at the dimerization interface (15). In this study, we used site-directed mutagenesis to demonstrate that the species specificity of MD-2 recognition of lipid IV_A is determined by surface charge differences at two specific areas: residues 122 and 125 near the hydrophobic pocket entrance, and residues 42 and 69 at the A patch opposite the dimerization interface (Fig. 9).

The roles of residues 122 and 125 in lipid IV_A activation are easy to understand. Because residue 122 resides at the hydrophobic pocket entrance, its surface charge can directly influence lipid IV_A binding. The side chain of Glu-122 (from mMD-2) carries strong negative charges that would repulse the similarly negatively charged phosphate on lipid IV_A to raise the 4′-phosphate (Fig. 2*a*). This change in orientation would permit ionic interactions between the 4′-phosphate on lipid IV_A and the positively charged patch at the mTLR4′ dimerization interface to trigger receptor dimerization. When murine Glu-122 was mutated to its human counterpart Lys-122, the positively charged side chain of Lys-122 attracted the negatively charged 4′-phosphate on lipid IV_A, forcing lipid IV_A down where it could not interact with the positively charged patch on mTLR4′ to trigger dimerization and reducing lipid

IV_A responsiveness. Because WT hMD-2 naturally has Lys-122 at this position, lipid IV_A does not activate proinflammatory responses when hMD-2 is present. However, gain of negative charges at the entrance of the hMD-2 hydrophobic pocket alone (by K122E mutation) were not sufficient to convert hMD-2 into a mouse phenotype. Loss of positive charges at the dimerization interface (K125L mutation), and at the A patch (R69G and Y41F mutations) (Fig. 9) were also required for a strong proinflammatory responses to lipid IV_A.

Leu-125 likely affects lipid IV_A activation through a direct effect on receptor dimerization (Fig. 9). Leu-125 sits on the Phe-126 loop, which is essential for receptor dimerization (13, 14). However, Phe-126 does not directly bridge dimerization in the hTLR4·hMD-2·LPS co-crystal structure (12); it actually folds back toward hMD-2 to accommodate the extra acyl chain of LPS that lies on hMD-2 surface in the co-crystal structure (12). Extensive hydrophobic interactions are observed among the extra acyl chain of LPS, hydrophobic residues on hMD-2 (Phe-126, Ile-124, Leu-87, Met-85, and Val-82), and hydrophobic residues on hTLR4′ (Phe-440′, Leu-444′, and Phe-463′) at the dimerization interface. Another interpretation, however, is that hydrophobic residues on MD-2 and TLR4′ at the dimerization interface form a hydrophobic pocket to fit in the extra acyl chain of LPS lying on hMD-2 surface. Whether this extra acyl chain simply has a volume effect or actually plays a functional role is not known.

This scenario is changed in the case of lipid IV_A activation by the mTLR4·mMD-2 complex. Although mTLR4 has the same hydrophobic residues (Phe-438′, Leu-442′, and Phe-461′) at the dimerization interface as hTLR4 (Phe-440′, Leu-44′, and Fhe-463′), mMD-2 has hydrophobic Leu-125 in place of positively charged Lys-125 on hMD-2, whereas lipid IV_A has four acyl chains instead of six in LPS. Therefore, the hydrophobicity of the mMD-2 Phe-126 loop is increased, but lipid hydrophobicity is decreased. Leu-125 can coordinate with Phe-126 and Ile-124 on mMD-2 to interact with Met-417′, Phe-438′, Leu-442′, and Phe-461′ on mTLR4 through hydrophobic interactions (Fig. 2*a*), partially compensating for the reduced hydrophobic interactions due to the loss of two acyl chains in lipid IV_A.

The roles of Gly-69 and Phe-41 in lipid IV_A activation are likely to be indirect: these residues reside at the A patch opposite the dimerization interface (Fig. 9) and in the mTLR4·mMD-2 co-crystal structure, neither one is involved directly in the A patch interaction with mTLR4 (Fig. 4*d*) (13, 15). However, Gly-69 and Phe-41 are next to the two positively charged residues on mMD-2 (Arg-68 and Lys-109) that interact extensively with mTLR4 at the A patch of the mouse complex (Fig. 4*d*) (13). A similar interaction network was observed between hMD-2 and hTLR4 at the A patch in the hTLR4·hMD-2·LPS co-crystal structure (Fig. 4*c*) (12). Unlike F41 on mMD-2 that does not participate in the A patch interaction, Tyr-41 on hMD-2 is directly involved in hydrogen bonds with Glu-42 from hTLR4. Arg-69, on the other hand, sits next to Arg-68 on the same loop (Fig. 4*c*). Because both Arg-69 and Arg-68 are positively charged, the electrorepulsive forces between them will force the two side chains apart, pushing Arg-68 closer to Glu-42 on hTLR4 and freeing room for Tyr-41 on hMD-2 to interact with Glu-42 on hTLR4 through hydrogen bonds. Because Tyr-41 resides on a separate loop connected to the β3 strand instead of the β7 strand containing Arg-68, the gain of a hydrogen bond at this position likely has a global orientation effect on hMD-2 that requires extra forces to trigger receptor dimerization. Because lipid IV_A has only four acyl chains and does not have the core polysaccharide, it cannot activate the LPS receptor in the presence of hMD-2.

In fact, we suspected that the A patch residues on MD-2 would play a role in lipid IV_A discrimination because the relative orientations of hMD-2 and hTLR4 are different in the inhibitor-bound state (13) and the agonist-bound state (12). Prior to publication of the hTLR4·hMD-2·LPS co-crystal structure (PDB code 3FXI), Lee and co-workers had published the co-crystal structure of the TV3·hMD-2·Eritoran complex (PDB code 2Z65), which has the TLR4-hagfish fusion protein in place of intact ectodomain of hTLR4 (13). Both hMD-2 and the N-terminal 200 residues of hTLR4 are present in both crystal structures. However, when the two co-crystal structures are aligned on those hTLR4 N-terminal residues, the relative orientations of hMD-2 are different (supplemental Fig. 6). The hydrophobic pocket of MD-2 is tilted 6.7 Å (8.5°) farther away from TLR4 in inhibitor-bound TV3·hMD-2·Eritoran than it is in agonist-bound hTLR4·hMD-2·LPS. It is likely that LPS binding triggered a global orientation event between hMD-2 and hTLR4 to facilitate receptor dimerization, due to the strong hydrophobic interactions at the dimerization interface from the extra acyl chain. Although we cannot exclude the possibility that the different tilt angles between the two crystal structures merely result from the replacement of hTLR4 with TV3 in the inhibitor-bound state, the observation that charge mutation of the MD-2 A patch affects lipid IV_A activation strongly argues against this possibility.

Lipid IV_A is a partial agonist in equine cells (19). However, similar to human MD-2, equine MD-2 has the positively charged Arg-122 at the hydrophobic pocket entrance. Therefore, repulsive forces cannot be generated at the pocket entrance between Arg-122 and the lipid IV_A phosphate to lift lipid IV_A up. However, equine MD-2 has Ser-42 instead of murine Phe-42 or human Tyr-42 at the A patch. This substitution from aromatic residue to serine removes not only the hydrogen bond involving the hydroxyl group on Tyr-42 in the human receptor complex, but also any potential hydrophobic interactions with the aromatic ring in both human and mouse receptor. Consequently, the relative binding angle/rigidity between equine MD-2 and equine TLR4 could be substantially different from the other two species. Hence, lipid IV_A functions as a partial agonist in the presence of equine TLR4·MD-2 receptor.

A practical application of our finding here, however, is to extend this knowledge to the understanding of receptor polymorphisms. Species-specific recognition of lipid IV_A by the mouse and human TLR4·MD-2 receptor can be interpreted as two extreme cases of receptor polymorphism resulting in either complete activation or complete inhibition. Charge variation at a single residue can alter the response to lipid IV_A stimulation. Single nucleotide polymorphisms at TLR4 residues 299 and 399 reportedly decrease the proinflammatory response to LPS stimulation (20). Because these residues do not directly affect recep-

tor dimerization (supplemental Fig. 7), these single nucleotide polymorphisms may alter the relative binding angle/rigidity of the TLR4/MD-2 complex so that receptor dimerization is not as easily triggered by LPS cross-linking.

In conclusion, we used site-directed mutagenesis studies to demonstrate that induced changes in the three major forces at the dimerization interface, ionic interactions, hydrogen bonds, and hydrophobic interactions, contribute significantly to receptor function and explain the species specificity of LPS-binding responses. Different lipid A analogs that vary in acyl chain length or composition, or phosphate composition of the diglucosamine backbone, likely have different balances among the stabilizing forces at the dimerization interface that affect receptor dimerization and activation.

REFERENCES

1. Raetz, C. R., and Whitfield, C. (2002) *Annu. Rev. Biochem.* **71,** 635–700
2. Raetz, C. R., Reynolds, C. M., Trent, M. S., and Bishop, R. E. (2007) *Annu. Rev. Biochem.* **76,** 295–329
3. Golenbock, D. T., Hampton, R. Y., Qureshi, N., Takayama, K., and Raetz, C. R. (1991) *J. Biol. Chem.* **266,** 19490–19498
4. Poltorak, A., He, X., Smirnova, I., Liu, M. Y., Van Huffel, C., Du, X., Birdwell, D., Alejos, E., Silva, M., Galanos, C., Freudenberg, M., Ricciardi-Castagnoli, P., Layton, B., and Beutler, B. (1998) *Science* **282,** 2085–2088
5. Shimazu, R., Akashi, S., Ogata, H., Nagai, Y., Fukudome, K., Miyake, K., and Kimoto, M. (1999) *J. Exp. Med.* **189,** 1777–1782
6. Wright, S. D., Ramos, R. A., Tobias, P. S., Ulevitch, R. J., and Mathison, J. C. (1990) *Science* **249,** 1431–1433
7. Qureshi, S. T., Larivière, L., Leveque, G., Clermont, S., Moore, K. J., Gros, P., and Malo, D. (1999) *J. Exp. Med.* **189,** 615–625
8. Hoshino, K., Takeuchi, O., Kawai, T., Sanjo, H., Ogawa, T., Takeda, Y., Takeda, K., and Akira, S. (1999) *J. Immunol.* **162,** 3749–3752
9. Schromm, A. B., Lien, E., Henneke, P., Chow, J. C., Yoshimura, A., Heine, H., Latz, E., Monks, B. G., Schwartz, D. A., Miyake, K., and Golenbock, D. T. (2001) *J. Exp. Med.* **194,** 79–88
10. Nagai, Y., Akashi, S., Nagafuku, M., Ogata, M., Iwakura, Y., Akira, S., Kitamura, T., Kosugi, A., Kimoto, M., and Miyake, K. (2002) *Nat. Immunol.* **3,** 667–672
11. Perera, P. Y., Vogel, S. N., Detore, G. R., Haziot, A., and Goyert, S. M. (1997) *J. Immunol.* **158,** 4422–4429
12. Park, B. S., Song, D. H., Kim, H. M., Choi, B. S., Lee, H., and Lee, J. O. (2009) *Nature* **458,** 1191–1195
13. Kim, H. M., Park, B. S., Kim, J. I., Kim, S. E., Lee, J., Oh, S. C., Enkhbayar, P., Matsushima, N., Lee, H., Yoo, O. J., and Lee, J. O. (2007) *Cell* **130,** 906–917
14. Resman, N., Vasl, J., Oblak, A., Pristovsek, P., Gioannini, T. L., Weiss, J. P., and Jerala, R. (2009) *J. Biol. Chem.* **284,** 15052–15060
15. Meng, J., Lien, E., and Golenbock, D. T. (2010) *J. Biol. Chem.* **285,** 8695–8702
16. Hirschfeld, M., Ma, Y., Weis, J. H., Vogel, S. N., and Weis, J. J. (2000) *J. Immunol.* **165,** 618–622
17. Fitzgerald, K. A., Palsson-McDermott, E. M., Bowie, A. G., Jefferies, C. A., Mansell, A. S., Brady, G., Brint, E., Dunne, A., Gray, P., Harte, M. T., McMurray, D., Smith, D. E., Sims, J. E., Bird, T. A., and O'Neill, L. A. (2001) *Nature* **413,** 78–83
18. Ohto, U., Fukase, K., Miyake, K., and Satow, Y. (2007) *Science* **316,** 1632–1634
19. Walsh, C., Gangloff, M., Monie, T., Smyth, T., Wei, B., McKinley, T. J., Maskell, D., Gay, N., and Bryant, C. (2008) *J. Immunol.* **181,** 1245–1254
20. Awomoyi, A. A., Rallabhandi, P., Pollin, T. I., Lorenz, E., Sztein, M. B., Boukhvalova, M. S., Hemming, V. G., Blanco, J. C., and Vogel, S. N. (2007) *J. Immunol.* **179,** 3171–3177
21. Koradi, R., Billeter, M., and Wuthrich, K. (1996) *J. Mol. Graph. Model.* **14,** 29–32, 51–55

MD-2 Residues Tyrosine 42, Arginine 69, Aspartic Acid 122, and Leucine 125 Provide Species Specificity for Lipid IV $_A$

Jianmin Meng, Joshua R. Drolet, Brian G. Monks and Douglas T. Golenbock

J. Biol. Chem. 2010, 285:27935-27943.
doi: 10.1074/jbc.M110.134668 originally published online June 30, 2010

SI Figure legend

SI Figure 1. The electrostatic surface charges are similar between hMD-2 and mMD-2 at the B patch, and between hTLR4 and mTLR4 at both the A and B patches. Electrostatic surface charges were calculated for hMD-2, mMD-2, hTLR4, and mTLR4 in MolMol (1). Surface charges of hMD-2 (left) and mMD-2 (right) at the B-patch are shown in (a), surfaces charges of hTLR4 (left) and mTLR4 (right) at the B patch are shown in (b), and surfaces charges of hTLR4 (left) and mTLR4 (right) at the A patch are shown in (c). The A and B patches are circled and labeled. Red for negatively charged surface, blue for positively charged surface, and white for non-charged surface.

SI Figure 2. The hMD-2 double mutant, R69G_K122E, gained most lipid IV_A responsiveness among all double mutants. HEK293 cells were transiently tranfected with: 1) one of the ten hMD-2 double mutants; 2) mTLR4 wild type construct; 3) a NF-κB-luciferase reporter construct; 4) a renilla-luciferase reporter construct. After overnight transfection, cells were stimulated with 1000 ng/ml, 100 ng/ml, 10 ng/ml, or 0 ng/ml of LPS (a) or lipid IV_A (b) overnight. Supernatants were then removed, and NF-κB-luciferase was measured in cell lysates. The luciferase shown has been normalized by renilla-luciferase. Data are one representative figure of three replicates.

SI Figure 3. The hMD-2 quadruple mutant, Y42F_R69G_K122E_K125L, gained most lipid IV_A responsiveness among all mutants. The high-order hMD-2 mutants were transiently transfected with wild type mTLR4 and reporter constructs overnight, and stimulated with decreasing concentrations of LPS (a) or lipid IV_A (b) as described in SI

Fig. 2. The next day, supernatants were removed, and NF-κB-luciferase was measured in cell lysates. The luciferase shown has been normalized by renilla-luciferase. One representative data from three replicates are shown in the figure.

SI Figure 4. The mMD-2 double mutants that contain the E122K mutation lost most of the lipid IV_A responsiveness. The ten mMD-2 double mutants were transiently transfected with mTLR4 to HEK293 cells, along with an NF-κB luciferase reporter construct and renilla-luciferase reporter construct. After overnight transfection, cells were stimulated with 1000 ng/ml, 100 ng/ml, 10 ng/ml, or 0 ng/ml lipid IV_A (a) or LPS (b). The next day, supernatants were removed, and NF-κB-luciferase was measured in cell lysates. The luciferase shown has been normalized by renilla-luciferase. Data are one representative figure of three repeating experiments.

SI Figure 5. The high-order mMD-2 mutants that contain the E122K mutations lost most of the lipid IV_A responsiveness. The triple and quadruple mutants that contain both E122K and L125K mutations were transiently transfected with mTLR4 to HEK293 cells, along with an NF-κB luciferase reporter construct and renilla-luciferase reporter construct. After overnight transfection, cells were stimulated with 1000 ng/ml, 100 ng/ml, 10 ng/ml, or 0 ng/ml lipid IV_A (a) or LPS (b). The next day, supernatants were removed, and NF-κB-luciferase was measured in cell lysates. The luciferase shown has been normalized by renilla-luciferase. Data are one representative figure of three repeating experiments.

SI Figure 6. The hydrophobic pocket of hMD-2 is tilted away from TLR4 in the Eritoran-bound state vs. the LPS-bound state. The co-crystal structures of TV3/hMD-2/Eritoran (PDB ID: 2Z65) (2) and hTLR4/hMD-2/LPS (PDB ID: 3FXI) (3) were aligned on the N-terminal 200 residues of hTLR4. The tilt angle and distance of hMD-2 in the two structures are labeled. Color scheme: hTLR4 in 3FXI (pink), hMD-2 in 3FXI (brown); TV3 in 2Z65 (light yellow), hMD-2 in 2Z65 (green).

SI Figure 7. I299 and L399 in the hTLR4/hMD-2/LPS co-crystal structure. The hTLR4/hMD-2/LPS co-crystal structure (PDB ID: 3FXI) (3) was shown in two perpendicular views. The single polymorphism residues (SNPs) of I299 and L399 are shown as black spheres and labeled. Color scheme: hTLR4 (light pink), hMD-2 (hot pink), LPS (cyan); hTLR4' (wheat), hMD-2' (magenta), LPS' (green).

SI References:

1. Koradi, R., M. Billeter, and K. Wuthrich. 1996. MOLMOL: a program for display and analysis of macromolecular structures. *J Mol Graph* 14:51-55, 29-32.
2. Kim, H. M., B. S. Park, J. I. Kim, S. E. Kim, J. Lee, S. C. Oh, P. Enkhbayar, N. Matsushima, H. Lee, O. J. Yoo, and J. O. Lee. 2007. Crystal structure of the TLR4-MD-2 complex with bound endotoxin antagonist Eritoran. *Cell* 130:906-917.
3. Park, B. S., D. H. Song, H. M. Kim, B. S. Choi, H. Lee, and J. O. Lee. 2009. The structural basis of lipopolysaccharide recognition by the TLR4-MD-2 complex. *Nature*.

Meng et al, SI Figure 1

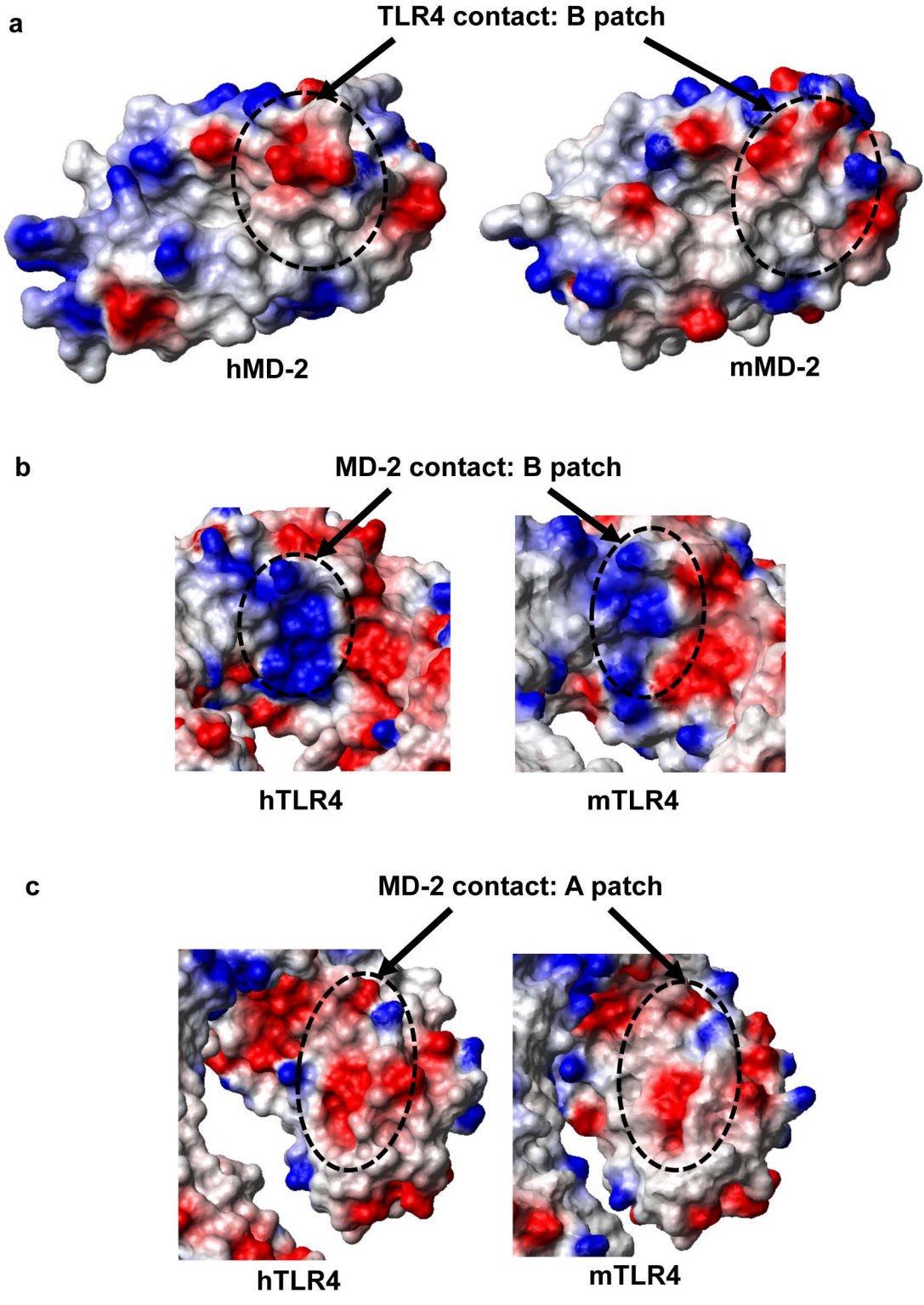

Meng et al, SI Figure 2

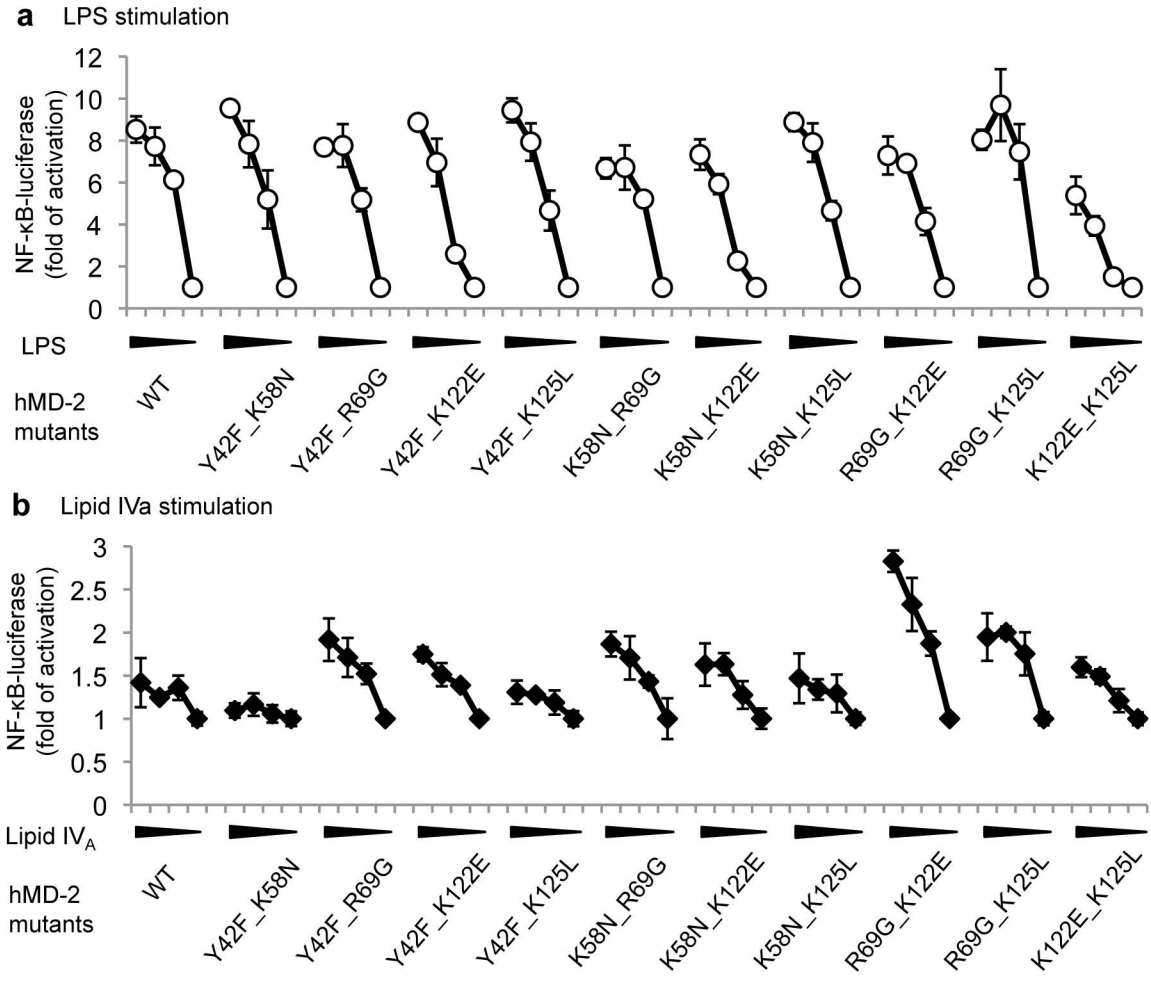

Meng et al, SI Figure 3

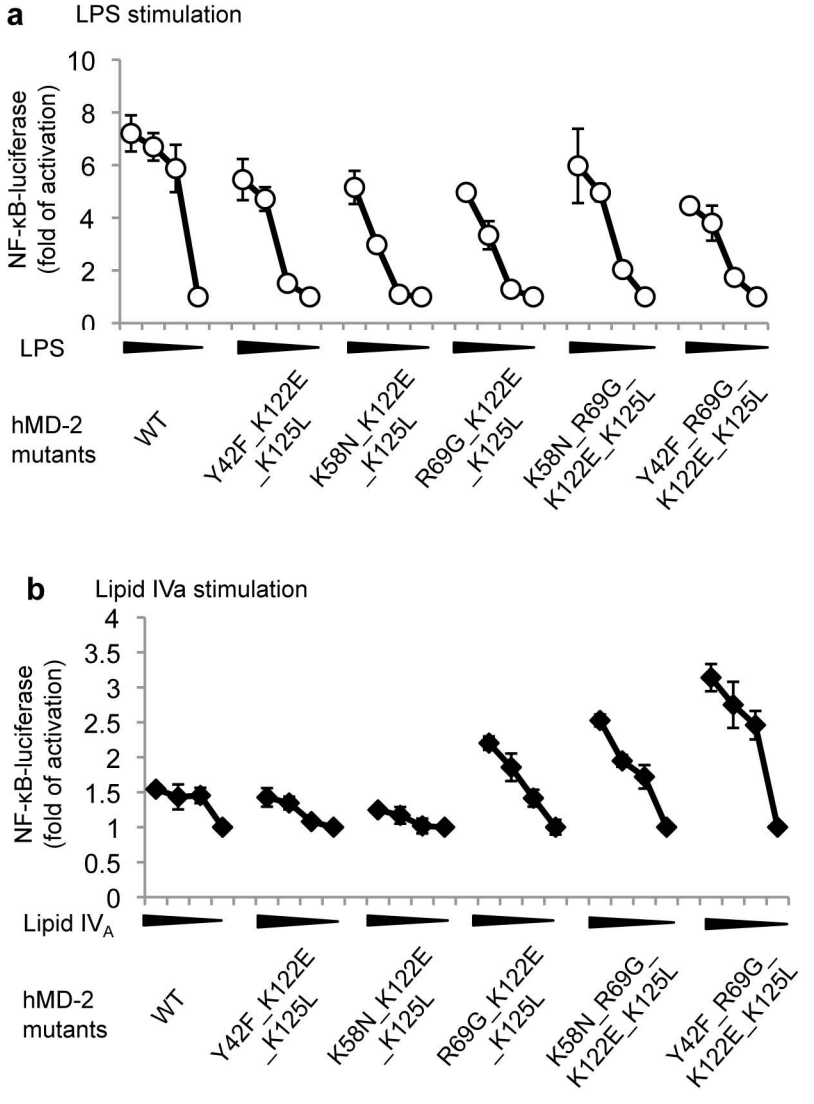

Meng et al, SI Figure 4

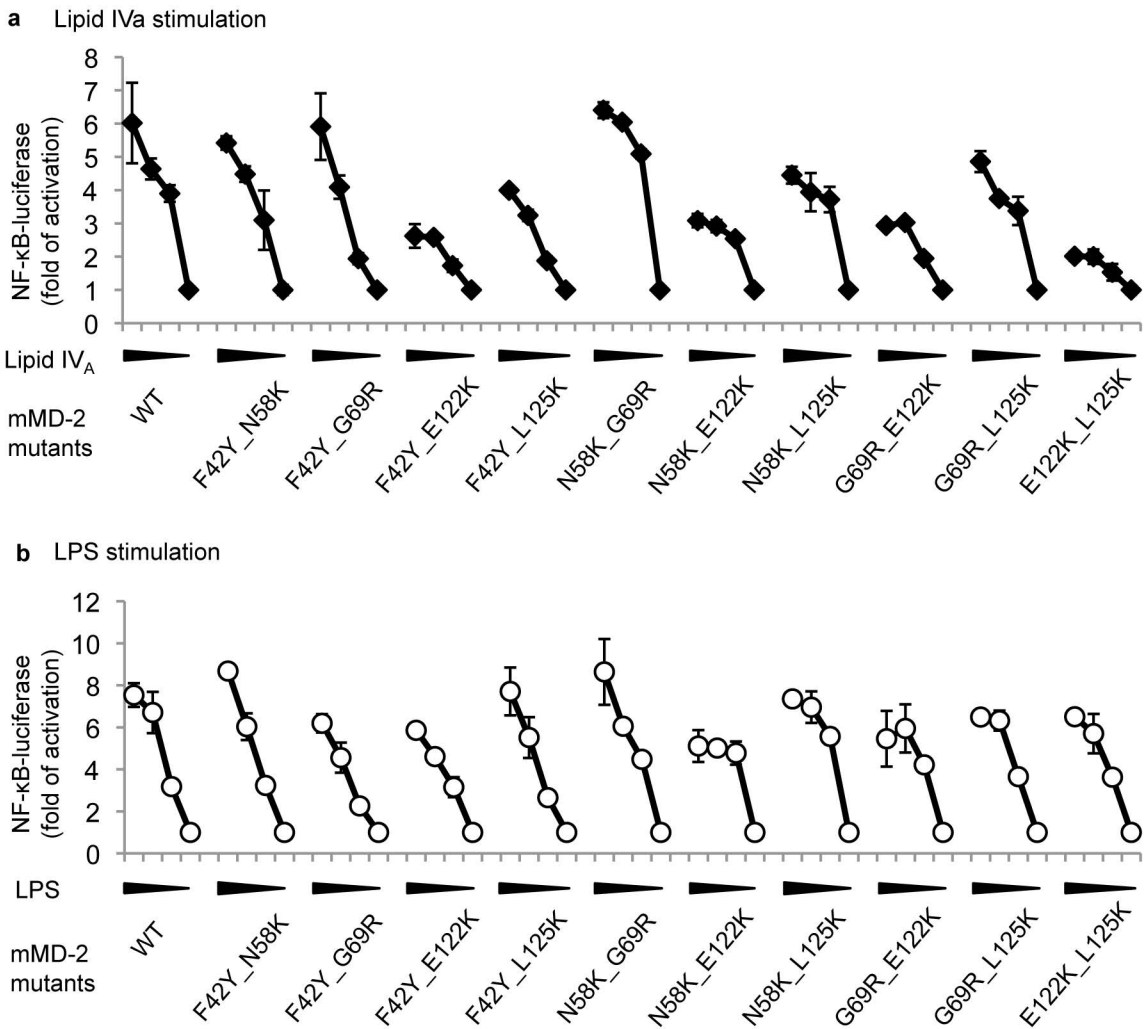

Meng et al, SI Figure 5

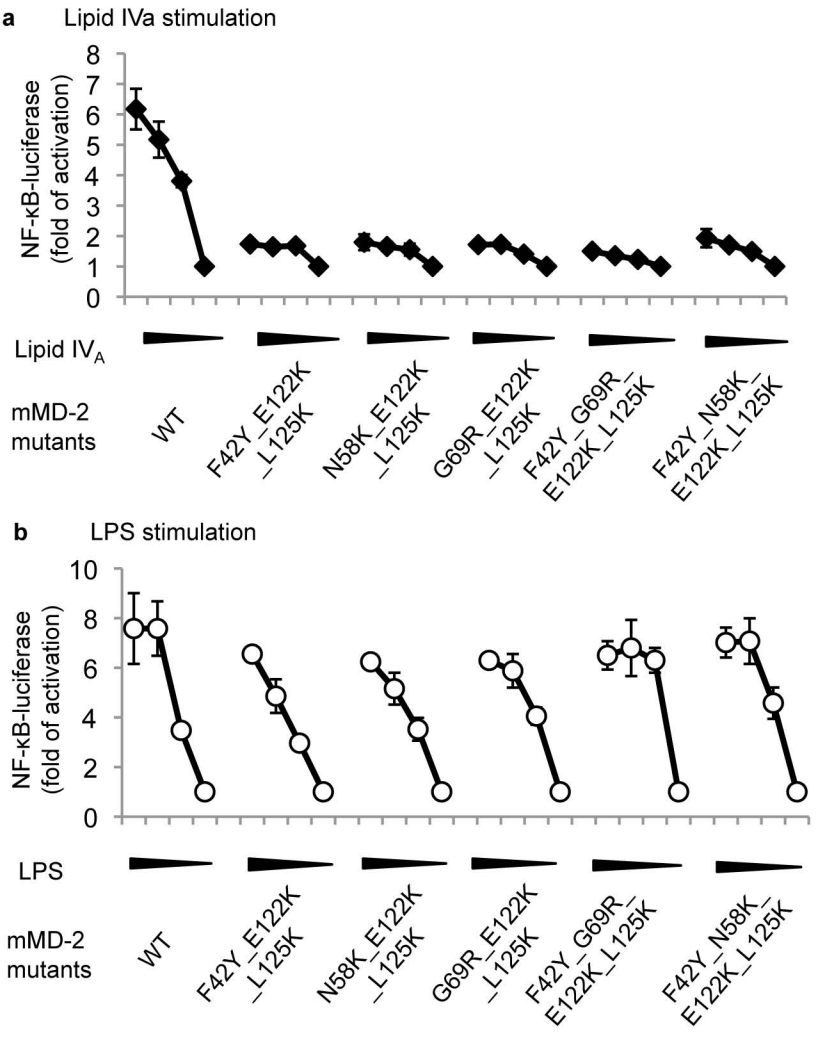

Meng et al, SI Figure 6

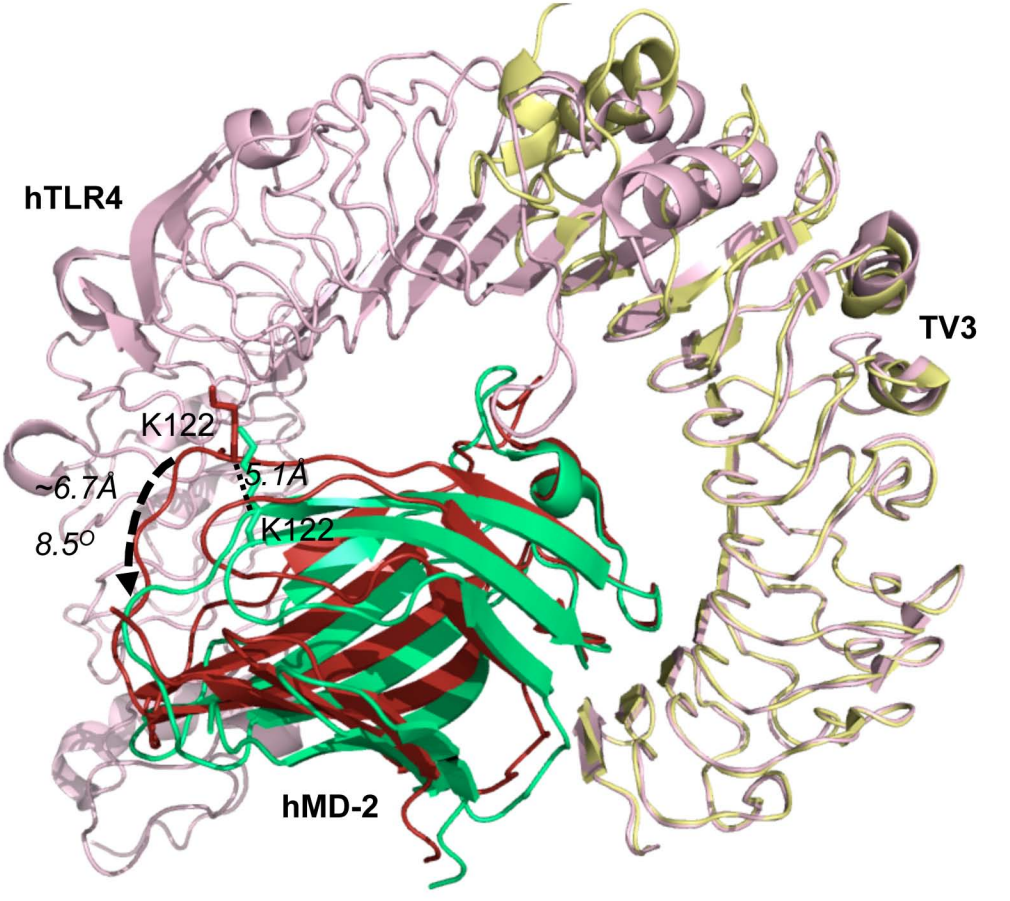

Meng et al, SI Figure 7